NOTE

Promotion of angiogenesis toward transplanted ovaries using nitric oxide releasing nanoparticles in fibrin hydrogel

Biofabrication

NOTE

RECEIVED
29 March 2021

REVISED
12 November 2021

ACCEPTED FOR PUBLICATION
1 December 2021

PUBLISHED
29 December 2021

Promotion of angiogenesis toward transplanted ovaries using nitric oxide releasing nanoparticles in fibrin hydrogel

Chungmo Yang[1,2], Nanum Chung[1,3], Chaeyoung Song[1,3], Hye Won Youm[1], Kangwon Lee[4,*] and Jung Ryeol Lee[1,3,5,*]

[1] Department of Obstetrics and Gynecology, Seoul National University Bundang Hospital, Seongnam 13620, Republic of Korea
[2] Program in Nanoscience and Technology, Graduate School of Convergence Science and Technology, Seoul National University, Seoul, 08826, Republic of Korea
[3] Department of Translational Medicine, Seoul National University College of Medicine, Seoul 03080, Republic of Korea
[4] Department of Applied Bioengineering, Graduate School of Convergence Science and Technology, Seoul National University, Seoul 08826, Republic of Korea
[5] Department of Obstetrics and Gynecology, Seoul National University College of Medicine, Seoul 03080, Republic of Korea
[*] Authors to whom any correspondence should be addressed.

E-mail: leejrmd@snu.ac.kr **and** kangwonlee@snu.ac.kr

Keywords: angiogenesis, fibrin hydrogel, nitric oxide-releasing nanoparticles, fertility preservation, ovarian transplantation

Supplementary material for this article is available online

Abstract

Transplantation of ovary is one method of facilitating fertility preservation to increase the quality of life of cancer survivors. Immediately after transplantation, ovaries are under ischemic conditions owing to a lack of vascular anastomosis between the graft and host tissues. The transplanted ovaries can suffer damage because of lack of oxygen and nutrients, resulting in necrosis and dysfunction. In the technique proposed in this paper, the ovary is encapsulated with nitric oxide-releasing nanoparticles (NO-NPs) in fibrin hydrogels, which form a carrying matrix to prevent ischemic damage and accelerate angiogenesis. The low concentration of NO released from mPEG-PLGA nanoparticles elicits blood vessel formation, which allows transplanted ovaries in the subcutis to recover from the ischemic period. In experiments with mice, the NO-NPs/fibrin hydrogel improved the total number and quality of ovarian follicles after transplantation. The intra-ovarian vascular density was 4.78 folds higher for the NO-NPs/fibrin hydrogel groups compared to that for the nontreated groups. Finally, *in vitro* fertilization revealed a successful blastocyst formation rate for NO-NPs/fibrin hydrogel coated ovaries. Thus, NO-NPs/fibrin hydrogels can provide an appropriate milieu to promote angiogenesis and be considered as adjuvant surgery materials for fertility preservation.

1. Introduction

Fertility preservation has been implemented in female cancer patients, adolescents, transgender men, and individuals suffering from age-related fertility loss. Recently, cancer therapy has become more successful because of advances in the drug industry and surgical techniques worldwide [1, 2]. However, chemotherapy can affect reproductive organs by inducing gonadotoxicity [3]. Loss of fertility after cancer therapy can be a critical issue affecting the quality of life of cancer survivors. Ovarian tissue cryopreservation is an alternative fertility preservation method for female patients [4]. To date, numerous attempts have been made to improve ovarian function after frozen–thawed ovarian tissue transplantation (OTT) [5, 6]. Although successful ovarian functional recovery and live births have been reported [7–12], improving this technique remains necessary for better ovarian function and follicle survival. Ischemic injury is a major cause of ovarian damage because of the absence of vessels supplying oxygen and nutrients after OTT [13]. The main limitation of OTT (or whole ovary transplantation) is poor angiogenesis resulting from the difficulty in connecting blood vessels during the procedure.

Angiogenesis is the formation of new blood vessels by sprouting cells from pre-existing vessels. Successful angiogenesis and anastomosis are crucial to integrating transplanted tissues or scaffold. Enhancement of angiogenesis is the key to retrieving the function of ovaries because they are vulnerable to post-transplantation ischemia [14]. Several studies have revealed that angiogenesis induction helps with regaining reproductive functions and reducing ovarian damages after transplantation in mouse models using angiogenic factors [15, 16]. One of the endogenous gasotransmitters, NO can be synthesized using various nitric oxide synthases (NOS) in mammalian cells with stepwise oxidation of L-arginine. NO has been linked to angiogenesis, vasodilation, apoptosis, and antibacterial efficacy, depending on its concentration, emerging as sources for tissue engineering and clinical applications, which have involved in cyclic guanosine monophosphate (cGMP)-dependent or independent pathways [17–19].

Since angiogenesis can occur at a low level of NO and synthetic NO donors have burst release behavior, controlled release has been researched via biomaterials to facilitate its biological functions such as therapeutic angiogenesis [20]. For exogenous NO delivery, therapeutic angiogenesis can be efficiently and sustainably induced by polymeric carriers, for example, PLGA (poly(lactic-*co*-glycolic acid)), PEG (poly-ethylene glycol), PCL (poly(ε-caprolactone), and chitosan-based materials [21–24]. In particular, mPEG (methoxy PEG), PLGA, and their copolymer have been researched as polymeric carriers that can be applied to wound repair and the regeneration of vascular tissue and bone [25–27]. These regenerations can be achieved by prerequisite angiogenesis because of the importance of blood vessels to tissues. For example, a PEG-based hydrogel is a suitable ovarian tissue supporting materials [28, 29]. In addition, NO delivery considerably affects follicle development, oocyte competence, maturation, fertilization, aging, and embryo development [30].

Biocompatible polymers have been proposed as candidates for alternative tissue scaffolds, nano- or micro-sized vehicles for delivering bioactive molecules, and cell-laden materials for approaches in tissue engineering [19]. Polymer-based materials have been used as additives for enhancing the reproductive functions of ovarian tissue and follicles such as PEG, alginate, collagen, fibrin, and gelatin [31, 32]. Among these, fibrin products are well qualified for tissue engineering and have been approved for biomedical use by the U.S. Food and Drug Administration. The use of fibrin hydrogel in reproductive medicine is also the primary option, either as an additive to transplanted ovaries or for the fabrication of artificial ovaries. Fibrin hydrogel with vascular endothelial growth factors (VEGF) has been reported to encapsulate the transplanted ovaries, promoting angiogenesis and ovarian graft survival [33]. In addition, fibrin provides an appropriate milieu for surrounding the *in vitro* culture of ovarian follicles for fertility preservation [34, 35].

In general, polymeric nanoparticles embedded fibrin hydrogel can take advantage of the characteristics of nanoparticles and fibrin hydrogel. It is important to deliver the angiogenic factors locally at the transplanted ovaries to enable the transplants to regain their function as reproductive organ. Therefore, we utilized NO-releasing nanoparticles (NO-NPs) embedded in the fibrin hydrogel scaffold to induce angiogenesis to prevent ischemic damage in the initial period after ovarian transplantation in a mouse in this study (figure 1). The self-assembled NO-releasing mPEG-PLGA-NPs (methoxy poly(ethylene glycol)-*b*-poly(lactic-*co*-glycolic acid)-NPs) were prepared via a conventional double-emulsion method. Autotransplantation of the whole ovary with NO-NPs/fibrin hydrogels was implemented to investigate the effect of NO and fibrin hydrogels on the angiogenesis of the grafts.

2. Materials and methods

2.1. Materials

mPEG (MW 2000) and diethylenetriamine (DETA) NONOate (DETA NONOate acts as an NO donor.) were purchased from Acros Organics (Gael, Belgium). Tin (II) 2-ethylhexanoate, lactide, and glycolide were purchased from Sigma Aldrich (St. Louis, MO, USA). Polyvinyl alcohol (PVA) was obtained from Junsei Chemical (Tokyo, Japan). Fibrinogen and thrombin from human plasma were purchased from Sigma Aldrich (St. Louis, MO, USA). Other chemicals and organic solvents were purchased from Sigma Aldrich.

2.2. Preparation of nitric oxide-releasing mPEG-PLGA nanoparticles

The mPEG-PLGA copolymer and NO-releasing mPEG-PLGA nanoparticles were prepared according to previously reported methods [36]. The mPEG-PLGA copolymers were polymerized by ring-opening polymerization of lactide and glycolide, catalyzed by Tin (II) 2-ethylhexanoate (0.05 wt % of the total monomer), with mPEG as a macro initiator. The mPEG-PLGA NPs with DETA NONOate were prepared by a conventional double-emulsion method. In brief, the dried mPEG-PLGA copolymer (20 mg ml^{-1}) was dissolved in dichloromethane, mixed with the NO donor solution (5 wt% in 10 mM NaOH), and emulsified using a probe sonicator for 3 min. The emulsion was poured into 2% PVA solution and re-emulsified using the same method for 5 min. The emulsion mixed with 0.6% PVA solution was then vigorously stirred for 1 h at room temperature to evaporate the organic solvent. The nanoparticles were filtered and washed at least three times

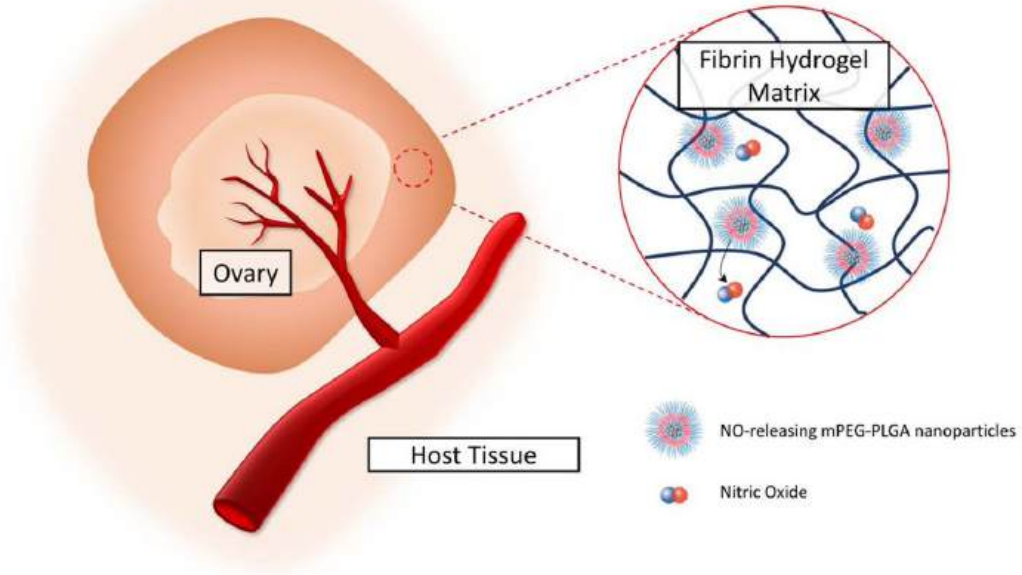

Figure 1. Schematic illustration of nitric oxide (NO)-releasing nanoparticles in fibrin hydrogel coated ovaries. The NO-releasing nanoparticles release NO in a fibrin hydrogel matrix to the periphery area of the ovaries, eliciting angiogenesis from host pre-existing vasculatures.

with deionized water. The obtained NO-NPs were lyophilized for 3 d and stored at −20 °C before use.

2.3. Characterizations of mPEG-PLGA copolymers and NO-NPs

2.3.1. Structural analysis by spectroscopy

The polymers were characterized using proton nuclear magnetic resonance spectrometry (^{1}H NMR; Bruker ADVANCE II 400, Billerica, MA, USA) with chloroform as a solvent to confirm the existence of mPEG-PLGA copolymer structures. Chemical shifts (δ value) were given in parts per million (ppm). A Fourier-transform infrared spectrometer (FTIR; SpectrumGX, Perkin-Elmer, Waltham, MA., USA) was used to measure the copolymer structure.

2.3.2. Morphological analysis and size distribution

The observation of the NPs was carried out using transmission electron microscopy (TEM; JEM-3100, Jeol Ltd, Japan). Negative staining with sodium phosphotungstic acid solution (1%) was conducted to pretreat the NPs. The size distribution was measured using a Zeta sizer (Malvern Instruments Ltd, Malvern, UK) with a fixed scattering angle of 173° at 25 °C, and all samples were dispersed in deionized water.

2.3.3. Measurement of NO release

NO levels from the NO-NPs were measured using a standard Griess assay with a nitrite/nitrate assay kit (Sigma-Aldrich, St. Louis, MO, USA) according to the manufacturer's protocol under normal physiological conditions. First, NO-NPs were dissolved in Dulbecco's phosphate buffered saline (DPBS, Biowest, Riverside, MO, USA). The mixture was placed in a dialysis bag (Cellu-Sep 5000 MWCO) to freely diffuse the NO. In the case of NO-NPs/fibrin hydrogel, fibrinogen and thrombin (containing NO-NPs) were put in the dialysis bag, then, the solution was carefully mixed. The dialysis bag was immersed in DPBS and maintained at 37 °C. At each time point, 100 μl of the sample were taken. Nitrate reductase and the enzyme cofactor, in an amount prescribed by instructions, were added to the solution, then, the samples were incubated at room temperature for 30 min with gentle shaking. The nitrate reductase reduces the nitrate to nitrite. Griess reagents were then added to the samples, which were incubated for 30 min with gentle orbital shaking. The total concentrations of nitrate and nitrite were determined by measuring the absorbance at 540 nm and computing the standard curve at different time points.

2.4. Preparation of NO-NPs/fibrin hydrogels and ovarian transplantation

Experimental procedures involving animals were performed with the approval of the Institutional Animal Care and Use Committee of Seoul National University

Bundang Hospital (Approval No. BA-1903-268-017-01). Ovariectomy and subcutaneous transplantation were performed using previously reported procedures [15, 16]. The anesthetized 7–8 week-old BDF-1 mice were bilaterally ovariectomized, and the ovaries were coated with the hydrogel before subcutaneous transplantation. The ovaries were washed with Dulbecco's phosphate buffered saline (DPBS) to eliminate blood and were immersed in thrombin solution (5 IU ml^{-1}) for 30 s. Then, the ovary in thrombin solution was transferred to fibrinogen (5 mg ml^{-1}) with or without NO-NP (0.1 mg ml^{-1}) solution for 1 min. This procedure was repeated twice before transplantation. To observe the structure of hydrogel-coated ovaries, the coated ovaries were immediately immersed in liquid nitrogen after the coating steps and freeze-dried for 3 d for SEM imaging.

2.5. Histological analysis

The transplanted ovaries were collected after 1, 3, 7, and 21 d (total 7 mice each group), and the tissues were fixed with 4% paraformaldehyde. The harvested ovaries were embedded in paraffin and sectioned (4 μm thickness). The serial sections were stained every fifth cut with hematoxylin and eosin (H&E) solution (Merck, Darmstadt, Germany) for histological evaluation. The other sections were used for immunohistochemistry (IHC) and terminal deoxynucleotidyl transferase dUTP nick end labeling (TUNEL) assays (Roche, Mannheim, Germany).

The H&E-stained ovaries were observed under a microscope (Carl Zeiss, Oberkochen, Germany), and the ovarian follicles in every fifth section were counted and classified into four developmental stages according to previously described criteria [15, 37]. The primordial follicles were designated with a single layer of flattened granulosa cells. Follicles with single-layered granulosa cells with one or more cuboidal structures were regarded as primary. With no antrum, the secondary follicles comprised two or more layers of cuboidal granulosa cells. Finally, antral follicles were classified with multiple layers of cuboidal granulosa cells and the antrum. For the morphological evaluation of follicle integrity, the following criteria were used to assess the follicles as grade 1, 2, or 3 (G1, G2, and G3). We evaluated the ovarian follicles in the transplanted ovaries with good and intact structures (G1), with intact oocytes and granulosa cells pulled away from the follicles (G2), and disrupted morphology and broken oocytes (G3).

2.6. Analysis of apoptosis

The apoptosis of the follicles and tissues was analyzed using the TUNEL assay (*In Situ* Cell Death Detection Kit Fluorescein, Roche, Mannheim, Germany) according to the manufacturer's protocol. The slides were incubated in a TUNEL reaction mixture (Enzyme solution: terminal deoxynucleotidyl transferase (TdT) and Label Solution: (fluorescein-dUTP)) for 1 h at 37 °C in a humidified dark chamber, after deparaffinization and rehydration. Then, the slides were mounted with a VECTASHIELD mounting medium with 4′,6-diamidino-2-phenylindole (DAPI; Vector Laboratories Inc., Burlingame, CA, USA) and examined with an inverted microscope (Zeiss AX10, Carl Zeiss, Oberkochen, Germany). Quantification of the apoptotic area in transplanted ovaries was analyzed using the ImageJ software (NIH, Bethesda, MD, USA).

2.7. Immunohistochemistry for CD31

The vascularity of the transplanted ovaries was investigated using immunohistochemistry with CD31. The unstained paraffin slides were deparaffinized and rehydrated. Then, the target retrieval solution was treated for antigenic retrieval. The sections were treated with a peroxidase-blocking solution, followed by incubation with an anti-CD31 antibody (1:200 dilution, Abcam, Cambridge, UK). After washing, the sections were treated with EnVision HRP and liquid DAB substrate (Dako Corp., Carpentaria, CA, USA), followed by counterstaining with hematoxylin. After dehydration, the slides were mounted and examined with an inverted microscope. To quantify the vascular density, CD31-positive areas were analyzed using the ImageJ software.

2.8. Serum hormone levels

A serum was obtained from whole blood collected using cardiac puncture and centrifugation. We analyzed follicle stimulating hormone (FSH) and 17β-Estradiol (E2) levels to evaluate ovarian function after transplantation. The hormone levels were measured using an enzyme-linked immunosorbent assay (ELISA) (Mouse/Rat Estradiol #ES1805-100, CALBIOTECH, El Cajon, CA., USA; and Mouse FSH #CSB-E06871m, CUSABIO, Houston, TX., USA).

2.9. Ovarian response to stimulation

To investigate the reproductive function of the transplanted ovaries, the ovarian weight was measured after ovarian stimulation using 7.5 IU of pregnant mare serum gonadotropin (PMSG) intraperitoneally. After 24 h, the transplanted ovaries were harvested and washed to weigh.

2.10. *In vitro* fertilization

After 21 d of transplantation, the female mice were intraperitoneally injected with 7.5 IU of PMSG. After 48 h, human chorionic gonadotropin (hCG, 7.5 IU) was injected intraperitoneally. The mice were sacrificed, and the ovaries were harvested 18 h after hCG injection in an M199 medium (20% fetal bovine serum [FBS] and 1% penicillin-streptomycin [PS]). The growing antral follicles were punctured using a 26 G syringe under a microscope. The oocytes

collected from cumulus-oocyte complexes (COCs) with hyaluronidase were matured *in vitro* in M199 medium supplemented with FBS, PS, FSH, and hCG for 8 h to obtain metaphase II oocytes (MII). The oocytes were then transferred to the human tubal fluid (HTF) medium for *in vitro* fertilization (IVF). The spermatozoa were incubated for 1 h at 37 °C and 5.5% CO_2 to allow capacitation after collection from the cauda epididymis. After *in vitro* maturation, insemination was performed for IVF by suspending 10 μl of sperm in the HTF medium containing oocytes. After 24 h, the embryos were washed with KSOM medium and transferred into a fresh KSOM medium with a mineral-oil covering.

Blastocysts were observed after 72 h and fixed with 4% paraformaldehyde for immunostaining of Octamer binding protein-4 (*Oct4*). The fixed blastocysts were permeabilized with 0.5% Triton X-100 and blocked with 3% bovine serum albumin (BSA). After washing, the *Oct4*(1:200 dilution; Abcam, Cambridge, UK) in 0.5% BSA were incubated overnight at 4 °C. Then, Alexa Fluor 488-conjugated secondary antibody (1:1000 dilution; Life Technologies, Grand Island, NY, USA) was incubated for 1 h at room temperature in the dark. The image analysis was conducted using a confocal microscope (LSM 800, Carl Zeiss, Oberkochen, Germany).

2.11. Quantitative reverse transcription polymerase chain reaction for analysis of gene expressions

Quantitative reverse transcription polymerase chain reaction (RT-qPCR) was used to confirm the gene expression of synthesized cDNA from the collected ovaries, using the primer (AccuTarget™ qPCR Screening kit, BIONEER Co., Daejeon, South Korea) and amfiSure qGreen Q-PCR Mater Mix (GenDEPOT, Barker, Tex., USA). RNA was extracted using TRIzol® (Invitrogen, Carlsbad, CA, USA). RT-qPCR using ViiA7 (Applied Biosystems, Life Technologies Corp., Carlsbad, CA, USA) was performed for angiogenesis-related genes (see Supplementary Materials), *FSHR*, and *Bax* with the reaction mixtures (20 μl). The initial step was predenaturation for 10 min at 95 °C, 40 cycles of 95 °C (5 s, denaturation), 58 °C (25 s, annealing), 72 °C (30 s, extension), and final extension for 5 min at 65 °C. The fold change in gene expression was calculated using the $2^{-\Delta\Delta Ct}$ method.

2.12. Statistical analysis

All data are represented in this paper as mean ± standard error of the mean (SEM). Statistically significant differences were analyzed by one-way or two-way analysis of variance (ANOVA) followed by Tukey's post hoc test or *t*-test using the GraphPad Prism software, version 6.0 (GraphPad Prism Software Inc., San Diego, CA, USA). A *P*-value less than 0.05 was considered statistically significant.

3. Results and discussion

3.1. Characterization of mPEG-PLGA and NO-NPs

The amphiphilic copolymer was linearly composed of mPEG and poly (lactic-*co*-glycolic) acid as hydrophilic and hydrophobic. mPEG-PLGA was synthesized by ring-opening polymerization of lactide and glycolide with mPEG, and tin (II) 2-ethylhexanoate functioned as a macroinitiator and catalyst (figure 2(a)). The FTIR and ^{1}H NMR spectra were analyzed to confirm the polymer structure (figures 2(b) and (c)). The characterization of PEG-PLGA copolymers achieved similar results to previous studies [38, 39]. The C=O and C–O stretching confirmed the bands at 1760 and 1090–1188 cm^{-1}. The C–H stretching of $–CH_2$ and C–H bonds was confirmed at 2995 and 2943 and 2875 cm^{-1}, respectively. The strong band at 3477 cm^{-1} indicated a stretch of the terminal hydroxyl group in the copolymer FTIR spectra. In the ^{1}H NMR spectra, the methylene protons in methoxy PEG and D- or -L-lactic acid repeat units were confirmed at δ 3.6 ppm and δ 1.55 ppm. In addition, the protons in $–CH_2–$ of lactic acid were observed at δ 4.8 ppm, and the protons in –CH– of lactic acid displayed δ 5.2 ppm.

The NO-NPs were prepared via the conventional double-emulsion method using a probe sonicator. After the NPs were dried, the nanoparticles showed a layered structure, as observed by TEM (figure 2(d)). The size and distribution of nanoparticles were observed approximately 160 nm (figure 2(e)). The sustained NO release from the mPEG-PLGA nanoparticles with or without fibrin hydrogel maintained a low level of NO for 48 h (figure 2(f)). NO release behavior can be slightly interfered by fibrin hydrogel matrix due to low concentration of fibrinogen and thrombin. Whereas, the DETA NONOate, as an NO donor encapsulated by mPEG-PLGA, exhibited a fast release of NO and high concentration within 10 h. These NO-NPs were confirmed to have angiogenic potentials using *in vitro* tube formation and *ex vivo* aorta ring assay in our previous report [36].

3.2. Preservation of transplanted ovaries by NO-NPs/fibrin hydrogels

To apply the nanoparticles in ovarian transplantation, we introduced fibrin hydrogel as a carrying matrix that supports and offers an appropriate environment to allow angiogenesis. The fibrin hydrogel matrix can provide a biocompatible milieu to transplanted ovaries in harsh subcutaneous conditions with no blood supply. We coated the ovaries with fibrin hydrogel with or without NO-NPs before transplantation, and the formation of a hydrogel-coated surface was confirmed by SEM (figure S1 (available online at stacks.iop.org/BF/14/011001/mmedia)). The transplanted ovaries in the subcutis were harvested 1, 3, 7, and 21 d after surgery (figure 3(a)). H&E staining of ovaries was used to estimate the number and

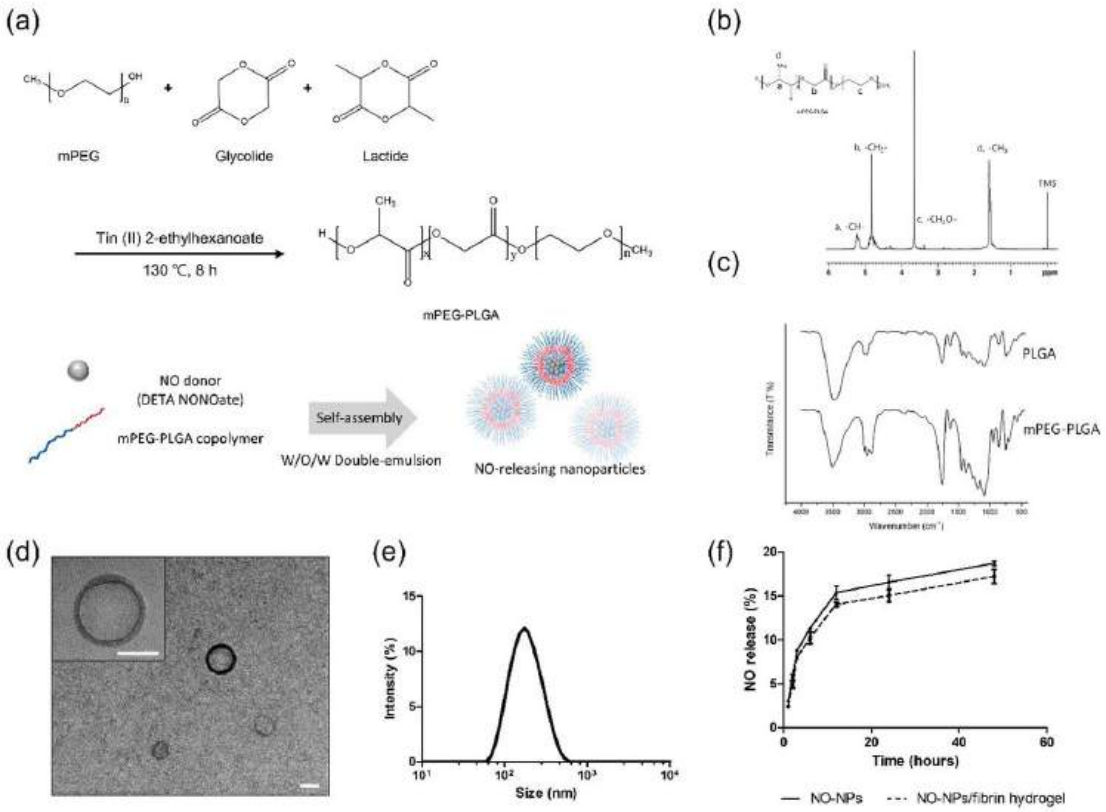

Figure 2. Synthesis scheme and characterization of mPEG-PLGA and NO-NPs: (a) polymerization of mPEG-PLGA from mPEG, lactide, and glycolide. Illustration of NO-NPs by the double-emulsion method containing DETA NONOate as the NO donor. Characterization of mPEG-PLGA by (b) ^{1}H NMR and (c) FTIR spectra. (d) TEM image of NO-NPs. The scale bars = 100 nm. (e) Size distribution of NO-NPs measured by DLS. (f) NO-releasing behavior of NO-NPs and NO-NPs/fibrin hydrogel.

structural quality of follicles. As shown in figure 3(b), the harvested ovaries exhibited squashed morphologies, damaged follicles, and cell-to-cell structures until day 3 in all experimental groups. However, the fibrin and NO-NPs/fibrin hydrogel-coated groups showed relatively high-graded follicles compared to the control group (non-treated). The total number of healthy follicles was greater in NO–NPs/fibrin hydrogel groups compared to the control or fibrin hydrogel alone (figure 3(c)). Likewise, the categorized follicles showed that treatment with fibrin or NO-NPs/fibrin hydrogels resulted in the maintenance of healthy or intact ovarian follicles in the subcutaneous milieu (figure 3(d)). The proportion of G1 follicles was 69.58 ± 2.661% from day 7 in the NO-NPs/fibrin hydrogel treatment group. After 21 d, the morphology and structure of tissues recovered healthy normality, even in the non-treated group; those of the fibrin and NO-NPs/fibrin hydrogel-coated groups were restored remarkably, similarly to normal tissue. The NO-NPs/fibrin hydrogel treatment resulted in 74.52 ± 2.509% of G1 ovarian follicles in the ovaries. In addition, fibrin hydrogel treatment enhanced the preserving effect after ischemic subcutaneous damage, and combined therapy using NO-NPs and fibrin hydrogel exhibited high efficacy in preserving ovarian follicles and tissue. The proportion of ovarian follicles in transplanted ovaries showed an increase of growing (secondary and antral) follicles until Day 7 in the control or fibrin hydrogel treatment groups (figure S2). However, the follicles in the NO–NPs/fibrin hydrogel group maintained the original proportions after transplantation. An ischemic environment activates ovarian follicles from dormant to growing follicles, and this is one of the causes of ovarian follicle loss after transplantation [37]. NO–NPs/fibrin hydrogel encapsulation prevented activation of follicles, and the proportion of growing follicles were maintained during the observation period after transplantation.

3.3. Evaluation of tissue apoptosis

After transplantation, the ovaries experience an ischemic milieu before new vessel formation. This ischemic period is a milestone that determines graft survival and functioning as a reproductive organ. Understandably, the ischemic milieu often results in apoptosis in the transplanted tissue because of oxygen deficiency caused by the lack of blood supply [40]. Ischemic injury is inevitable in transplanted ovaries, as shown in figures 4(a) and (b); in fact, the non-treated and transplanted ovaries exhibited severe apoptotic cell death (11.52 ± 0.31% at day 1, 26.89 ± 1.9% at day 3, and 30.2 ± 5.52% at day 7) in tissue analyzed by the TUNEL assay. The

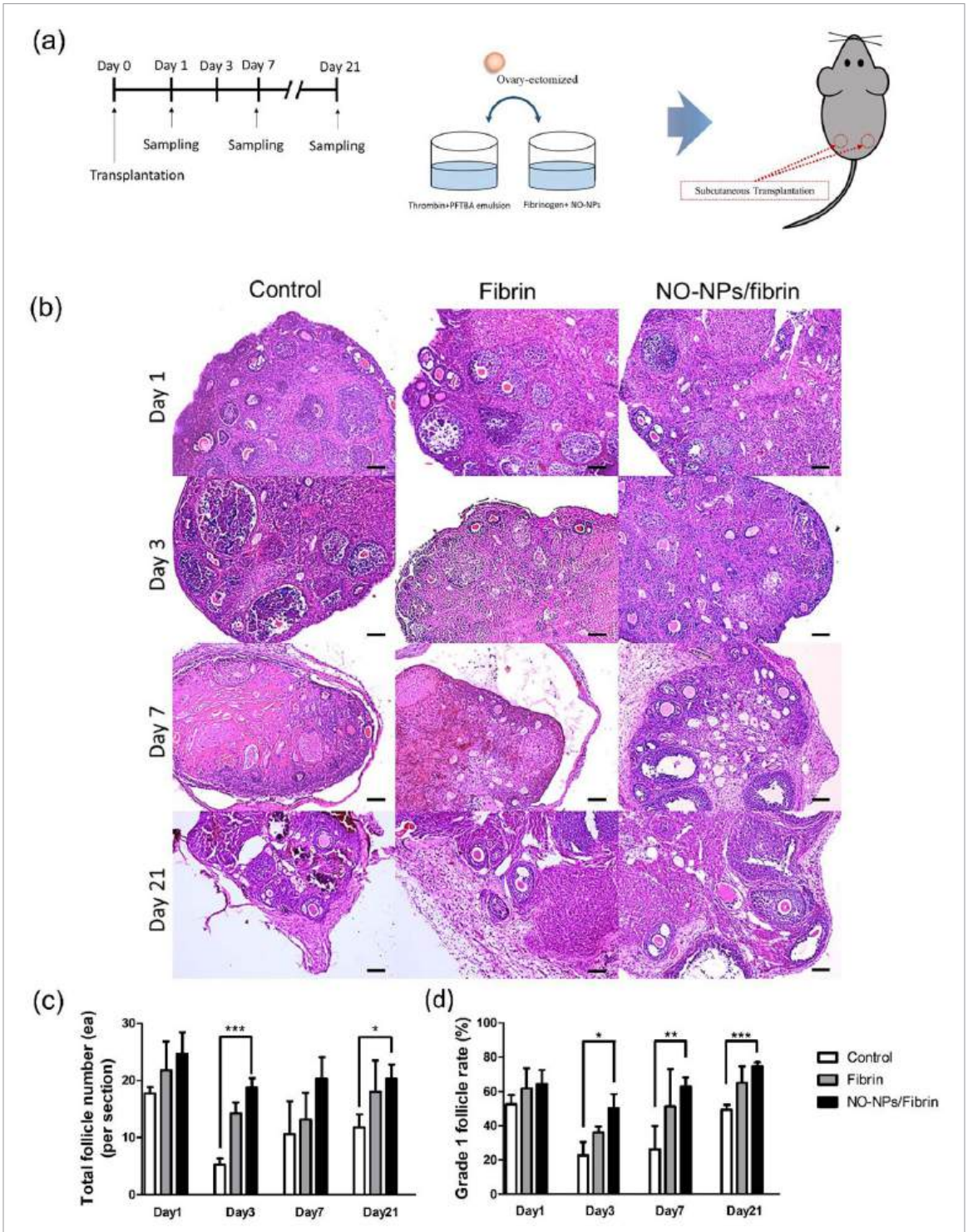

Figure 3. Histological analysis of transplanted ovaries: (a) experimental scheme with procedure of hydrogel coated ovaries. (b) H&E-stained ovaries after 1, 3, 7, and 21 d; the scale bars are 100 μm. (c) Total number and (d) grade of ovarian follicles in the control (non-treated), fibrin hydrogel, and NO-NPs/fibrin hydrogel groups (data are represented as the mean $\pm$ SEM; $n = 7$). $^{*}p < 0.05$, $^{**}p < 0.01$, and $^{***}p < 0.001$.

day after surgery, dead cells were observed at the center of the ovaries of the non-treated group. After 3 d, living cells were rarely observed in the center, and cells in the cortex were dying. By comparison, fibrin hydrogel-coated ovaries exhibited reduced dead cells at all time points. Fibrin hydrogel has been reported as a protective additive with transplantation or ovarian follicles to reduce apoptotic signals [33, 41]. The fibrin hydrogels with NO-NPs had a few dying cells in the tissue after transplantation. The quantification of the apoptotic area in NO-NPs/fibrin treatment was significantly low ($0.1674 \pm 0.0274\%$ at day 1, $0.4895 \pm 0.3020\%$ at day 3, $1.190 \pm 0.4866\%$ at day 7, and $0.5025 \pm 0.1129\%$ at day 21). Our results showed similar outcomes compared to the control groups. Remarkably, the non-treated control group exhibited

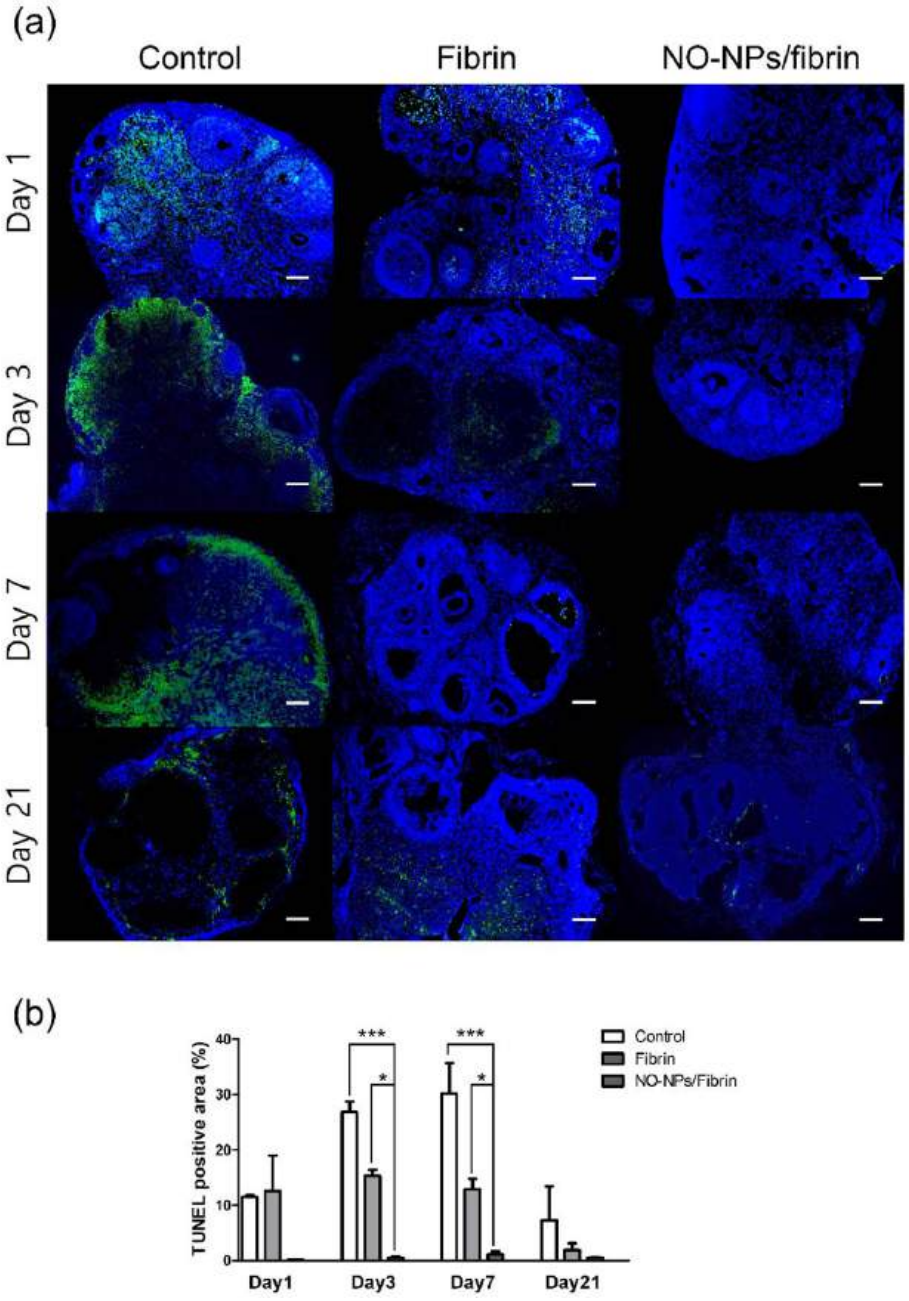

Figure 4. TUNEL assay of ovarian tissue: The TUNEL assay was conducted to evaluate apoptosis in ovarian tissue. (a) Green (FITC) indicates the TUNEL positive area, and blue (DAPI) indicates the cell nuclei. The scale bars are 100 μm. (b) Quantification of the TUNEL positive area in ovarian tissues (data are represented as the mean ± SEM; $n = 7$. $^{*}p < 0.05$ and $^{***}p < 0.001$).

severe DNA fragmentation, as shown in figure 4, in which the TUNEL-positive area resembled that of the fibrin hydrogel group 1 d after surgery. Severe DNA fragmentation was observed in the control groups 3 d later, whereas the fibrin hydrogel groups showed low TUNEL signals even after 3–7 d. This result suggests that the fibrin hydrogel can protect transplanted ovaries from ischemic damage. Three weeks later, the control group showed a relatively reduced apoptotic area at days 3–7. However, the apoptotic area was scarcely observed in NO-NPs with fibrin hydrogel, indicating that NO affects the ovarian and host tissues with fibrin hydrogel by a synergetic effect (figure 4).

3.4. Angiogenesis in transplanted ovaries

We assumed that the fibrin hydrogel and NO promote angiogenesis from the host subcutaneous tissue and ameliorate ischemic injury leading to follicle loss. In addition, the fibrin hydrogels act as a holding network for NO-NPs to enable local delivery. It was confirmed that H&E staining showed fewer or damaged follicles in the non-treated group, whereas those of the groups with fibrin hydrogel (with or without NO-NPs) improved (figure 3). This result implies that the early formation of blood vessels prevented ovarian follicle loss from the transplanted ovary. To prevent ischemic damage to transplanted

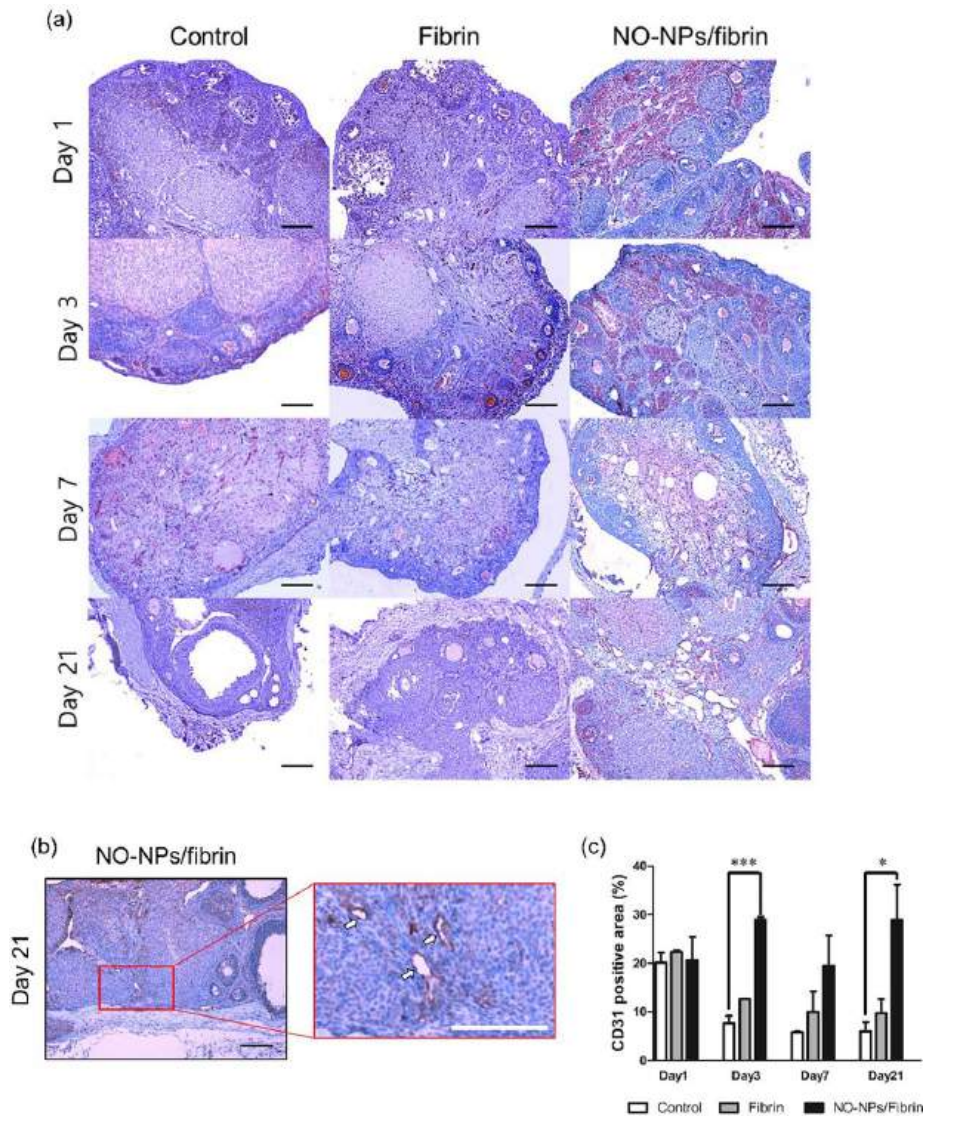

Figure 5. Immunohistochemistry of CD31 to analyze development vasculatures: (a) CD31 positive stain (brown, DAB) with counter-stain (hematoxylin). The scale bars are 100 μm. (b) blood vessel formation in ovarian tissue at day 21. The scale bar = 100 μm. (c) Quantification of CD31 (+) in ovarian tissues (data are represented as the mean ± SEM, $^{*}p < 0.05$).

ovaries, enhancement of angiogenesis to the transplanted tissue is essential for fertility preservation. CD31 immunohistochemistry allowed us to examine the relationship between vascular development and treated materials in the transplanted ovaries. The CD31 indicated endothelial cells composed of blood vessels in the ovary (figures 5(a) and (b)). CD31 was stained richly in the medulla part of the ovaries collected on day 1. At day 3, the NO-NPs/fibrin hydrogel-treated group exhibited considerable CD31 positive signals (28.99 ± 0.550%) compared to the control and fibrin hydrogel treated groups (7.645 ± 1.535% and 12.59 ± 0.085%, respectively). The CD31 positive areas were similar for all groups at day 1, whereas a difference was observed between the control and the fibrin- or NO-NP-treated groups after day 3. The NO treatment prominently showed CD31 positive cells in tissue compared to either the control or fibrin hydrogel groups. This result indicates that vigorous NO-induced angiogenesis occurred in the transplanted ovaries for 3 d. NO is involved in an initial step of angiogenesis by increasing the polarity of cells for preparing sprouts [42, 43]. After 7 d, the blood vessels were matured and partially observable in NO-treated mice. Thus, the successful restoration of reproductive function after transplantation by reducing the damage to the tissue or follicles is regulated by the tissue environment and eliciting formation of blood vessels. The vascular development was different from that of the NO-NPs/fibrin hydrogel (28.92 ± 7.235%) versus control (6.045 ± 1.845%) or fibrin hydrogel (9.720 ± 2.880%) groups 3 weeks post-surgery (figure 5(c)).

3.5. Ovarian response to stimulation and hormone (FSH and E2) levels in serum

Even when transplanted ovaries or follicles survive, they must regulate reproductive functions as

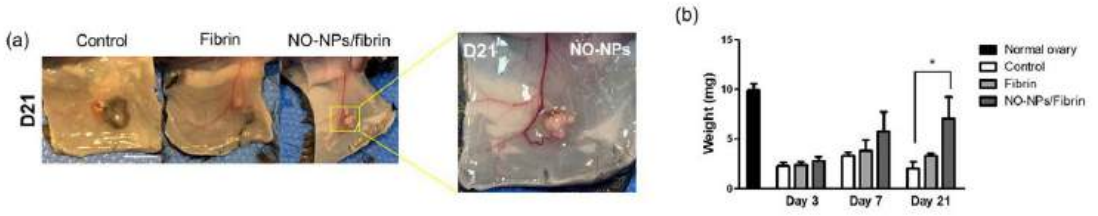

Figure 6. Ovarian response to PMSG stimulation: (a) optical images of subcutaneous transplanted ovaries at day 21. (b) Weight of ovarian tissues after PMSG stimulation after 24 h at days 3, 7, and 21 (data are represented as the mean ± SEM, $^{*}p < 0.05$).

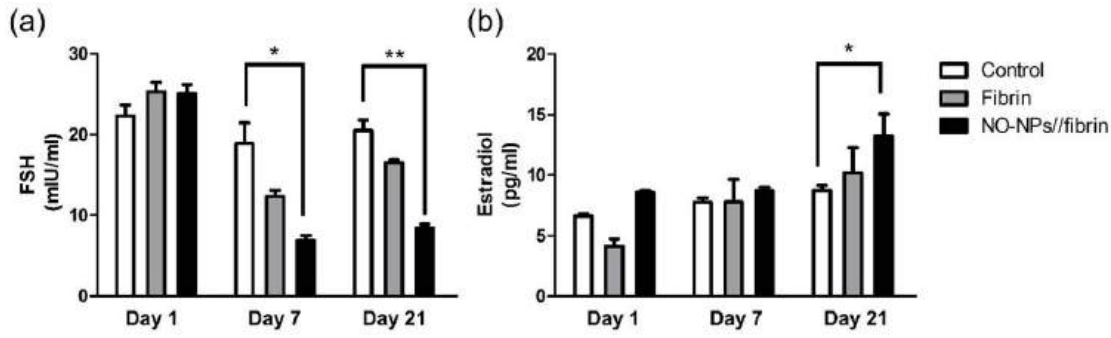

Figure 7. Hormone levels in serum: The serum FSH and Estradiol levels were analyzed by ELISA at day 1, 7, and 21. (a) The FSH level decreased after transplantation in the NO-NPs/fibrin hydrogel group, whereas (b) the Estradiol level was elevated (data are represented as the mean ± SEM; $^{*}p < 0.05$ and $^{**}p < 0.01$).

an organ. The ovary performs reproductive functions as well as endocrine functions with hormone production [44, 45]. If angiogenesis is successfully conducted from the host tissue to the transplanted ovaries, the ovaries can respond to gonadotropin stimulation. Ovarian weight after PMGS stimulation could be an indicator of ovarian reproductive function (figure 6). Before harvesting, the transplanted ovaries were observed in different sizes (figure 6(a)), which gradually increased during transplantation with NO-NPs/fibrin hydrogel treatment (figure 6(b)). The mass of fresh ovaries, collected from normal mice, averaged 9.925 ± 0.657 mg. The non-treated ovaries weighed 2.275 ± 0.357 and 3.3 ± 0.387 mg at days 3 and 7, respectively; the weight was lower than that of fresh ovaries even after 3 weeks (2.025 ± 0.687 mg). The fibrin hydrogel treated ovaries showed similar results: 2.4 ± 0.292, 3.8 ± 1.091, and 3.3 ± 0.280 mg at days 3, 7, and 21, respectively. The NO-NP treated ovaries exhibited results similar to those of the fresh ovaries. The ovaries weighed 2.775 ± 0.450 mg at day 3, with no significant difference from the other groups, but their weights increased remarkably until day 7, reaching 7.05 ± 2.189 mg after 3 weeks.

The ovariectomized mice exhibited increased FSH and decreased estradiol (E2) in the blood because of the loss of ovarian hormone production [46]. Retrieving hormone balance is evidence that our treatment successfully induces angiogenesis before losing the endocrine functions of the ovary [47, 48]. The serum hormone concentration is shown in figure 7. The FSH concentration in serum displayed a similar concentration in all experimental groups on day 1 (figure 7(a)). However, the fibrin hydrogel-treated groups showed suppressing behavior from day 7, and the NO-NPs additive group maintained a lower hormone level even 3 weeks after transplantation. In the case of E2, all experimental groups showed low levels until 1 week. However, the concentration of E2 in the NO-NPs/fibrin hydrogel-treated group increased 3 weeks later (figure 7(b)). The non-treated mice showed an increasing tendency of FSH, whereas E2 levels were reduced. This result indicates that the transplanted ovaries did not consume the FSH, which stopped production of E2. During transplantation, the mice had undergone an imbalance of sex hormones by anastomosis of the graft with host tissue, even after immediate auto-transplantation. All experimental groups showed similar levels of FSH and E2 on day 1. However, the FSH level increased in the non-treated or fibrin hydrogel groups and decreased in the NO-treated mice. Comparing these results with other results shows that angiogenesis in the transplanted ovaries was intensive owing to the controlled release of NO-NPs. After 21 d, the hormone levels in NO-treated mice showed the perinormal value of both FSH and E2 compared to those of non-treated mice. Thus, we considered that the NO-NPs/fibrin hydrogel-coated ovaries realized integrated blood vessels and exhibited feedback actions as a reproductive organ.

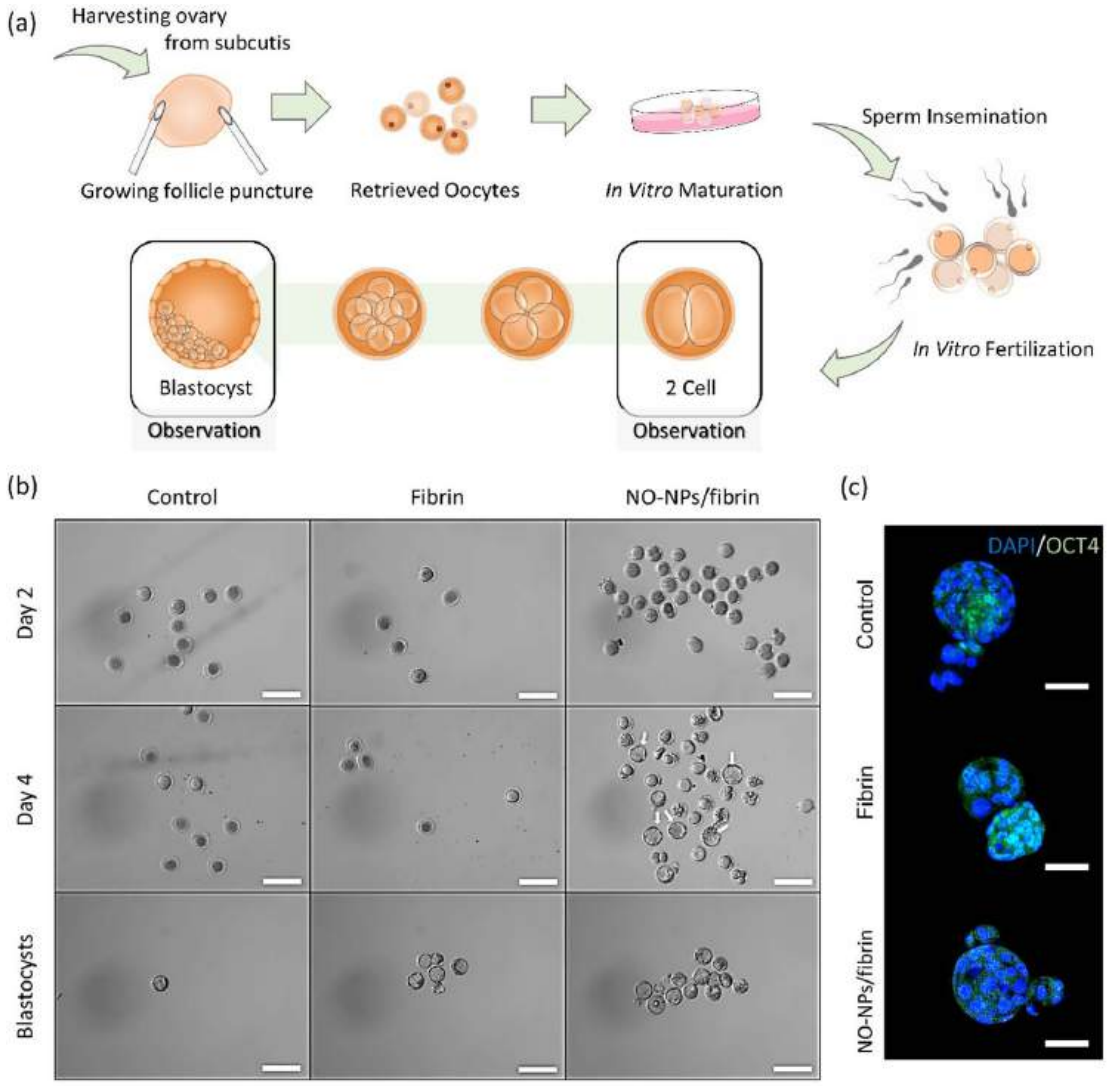

Figure 8. *In vitro* fertilization outcomes and immunocytochemistry of blastocysts (Oct4): (a) protocols *in vitro* fertilization harvested from transplanted mouse ovaries. (b) The retrieved oocytes developed to blastocysts (white arrows) at day 4 (scale bars = 200 μm). (c) Oct4 (green) and DAPI (blue) stained blastocysts (scale bars = 50 μm).

Table 1. IVF outcomes of oocytes from transplanted ovaries with non-treated (control), fibrin hydrogel, or NO-NPs/fibrin hydrogel.

Group	No. of mouse	No. of oocyte	Mean no. of oocyte	Maturation rate (%)	2 cell (%)	Blastocyst (%)
Control	5	37	2.47	6/37 (16%)	2/6 (33%)	1/2 (50%)
Fibrin hydrogel	5	58	3.87	19/58 (33%)	11/19 (58%)	4/11 (36%)
NO-NPs/fibrin	5	107	7.13	26/107 (24%)	18/26 (69%)	12/18 (67%)

3.6. *In vitro* fertilization

For fertility preservation, it is essential that fertilizable oocytes that can develop to blastocysts can be collected from the transplanted ovaries. Thus, we performed IVF to verify the feasibility of the proposed NO-NP treatment (figure 8(a)). As shown in figure 8(b) and table 1, IVF was performed to evaluate the fertility function of the transplanted ovaries (five mice per group). The non-treated mice exhibited 37 oocytes and 6 MII oocytes. In the case of the fibrin hydrogel group, 58 oocytes were collected from 19 MII oocytes. The MII oocyte rate was 16% and 33% in the non-treated and fibrin hydrogel groups, respectively. The NO-NPs/fibrin hydrogel treatment group exhibited 107 oocytes and a 24% MII rate. After insemination, the 2-cell or blastocyst development of the NO-NPs/fibrin hydrogel group was 69% or 67%, whereas the other values were 33% and 50% in the control or 58% and 36% in the fibrin hydrogel at day 4. To observe normality of blastocysts, we conducted immunostaining of *Oct4* (as a marker for embryonic stem cells) expression in blastocysts

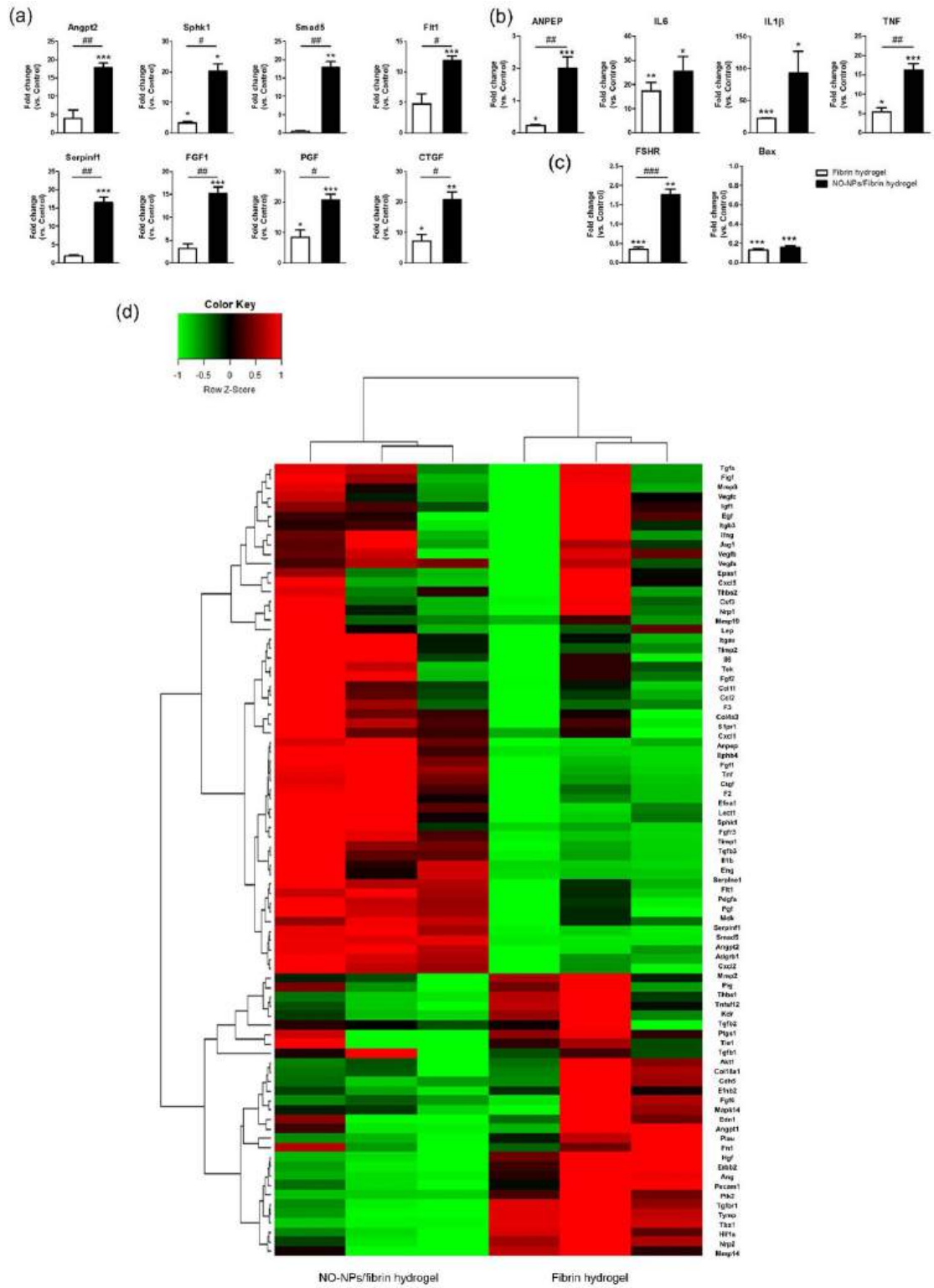

Figure 9. Gene expressions of angiogenic regulators, ovarian function, and apoptosis markers by RT-qPCR: (a) angiopoietin-2 (*Angpt2*), sphingosine kinase 1 (*Sphk1*), Mothers against decapentaplegic homolog 5 (*Smad5*), vascular endothelial growth factor receptor 1 (*Flt1; VEGFR1*), Serpin Family F Member 1 (*Serpinf1*), fibroblast growth factor 1 (*FGF1*), placental growth factor (*PGF*), and connective tissue growth factor (*CTGF*). (b) Membrane alanyl aminopeptidase (*ANPEP*), interleukin 1 beta (*IL-1β*), interleukin 6 (*IL-6*), and tumor necrosis factor (*TNF*). (c) Follicle-stimulating hormone receptor (*FSHR*) and Bcl-2-associated X protein (*Bax*). The fold changes represent gene expressions compared to those of the control. The screened-gene expressions present in (d) heatmap (data are represented as the mean ± SEM; p values: $^{*}p < 0.05$, $^{**}p < 0.01$, and $^{***}p < 0.001$ vs. Control; $^{\#}p < 0.05$, $^{\#\#}p < 0.01$, and $^{\#\#\#}p < 0.001$ Fibrin vs. NO-NPs/fibrin hydrogel.).

(figure 8(c)). The *Oct4* expression is in inner cell mass (ICM) and important to primitive endoderm specification [49, 50]. From the results, all blastocysts were found to be normal, regardless of treatment. These results suggest that angiogenesis induced by the NO-NPs/fibrin hydrogel improves the number of

oocyte and embryo development potential (figure 8). Early promotion of angiogenesis is the key to ovarian transplantation success with improved reproductive function. The controlled release of NO from the nanoparticles within the fibrin hydrogel promoted angiogenesis to protect ovaries from the ischemic environment. In addition, the relationship between oocyte and NO influenced this system [51]. As in the angiogenesis process, NO plays an important role in early reproduction steps at low concentrations, stimulating steroidogenesis and folliculogenesis [52]. Our treatment can influence the development of ovarian follicles and steroidogenesis inside transplanted ovaries and promote angiogenesis from host tissue to mitigate ischemic damage. The improved IVF outcomes of NO-treated ovarian grafts support the feasibility of this treatment for clinical application.

3.7. Gene expressions in transplanted ovaries

We analyzed gene expression 21 d after ovarian graft to evaluate successful establishment and progression of angiogenesis. Figure 9 shows the expression of angiogenesis-related genes in transplanted ovaries with fibrin or NO-NPs/fibrin hydrogel, upregulated compared to the control group (the total gene expression data are presented in table S1 and the scatter plot figure S3). The mRNA levels of several angiogenic factors were upregulated in the ovaries treated with NO-NPs/fibrin hydrogel compared to those with either control or fibrin hydrogel coating (figure 9). These factors include Angiopoietin-2 (*Angpt2*), Sphingosine kinase 1 (*Sphk1*), Mothers against decapentaplegic homolog 5 (*Smad5*), vascular endothelial growth factor receptor 1 (*Flt1; VEGFR1*), Serpin Family F Member 1 (*Serpinf1*), fibroblast growth factor 1 (*FGF1*), placental growth factor (*PGF*), and connective tissue growth factor (*CTGF*). The factors regulating angiogenesis and secretion by myeloid and lymphoid cells, such as membrane alanyl aminopeptidase (*ANPEP*), interleukin 1 beta (*IL-1β*), interleukin 6 (*IL-6*), and tumor necrosis factor (*TNF*), were also upregulated in the ovaries with NO-NPs/fibrin hydrogel treatment (figures 9(a) and (b)). In addition, *Bax* was downregulated in both fibrin-and NO-treated ovaries, indicating suppressed apoptotic signals in the grafts. The expression of Follicle-stimulating hormone receptor (*FSHR)*, an ovarian reserve marker, was upregulated solely in the NO-treatment groups (figure 9(c)). Once transplanted, the grafts experienced harsh conditions without blood supply, which occurred around the hypoxia-inflammatory-induced angiogenesis. Exogenous or endogenous NO expedites angiogenesis and modulates inflammation by inducing angiogenic factors, such as VEGF and bFGFs [53]. The performance of vascular development indicates that the ovaries remain alive and function as reproductive organs. We confirmed that the transplanted organ restored its function, and that the hydrogels settled down successfully with the host tissue and appropriate vasculature after 21 d. The gene expression of FSHR can indicate milestones restoring ovarian function after transplantation. The NO-NPs/fibrin hydrogels led to the proliferation of granulosa cells compared to fibrin hydrogel treatment, protecting the graft against the ischemic environment. In addition, the expression of Bcl-2-associated X protein (*Bax)*, a pro-apoptotic gene, was reduced in the fibrin hydrogel treatment with or without NO-NPs (figure 9(c)). This result indicates that the fibrin hydrogel has a protective effect on the transplanted tissue. The regulation of inflammation and angiogenesis genes is the key to the successful transplantation of biomaterials *in vivo*. Our data showed upregulated genes with inflammation–angiogenesis regulation, cell proliferation, and adhesions such as *Angpt2, Sphk1, Smad5, FGF1, Serpinf1, Flt1, PGF*, and *CTGF* (figure 9(a)). Together, the development of lymphatic vessels is indispensable in the ovary at the developmental stage and pathologies [54, 55]. One of the issues in tissue engineering is immunomodulation after transplantation of scaffolds *in vivo* [56]. The results showed that the expression of genes (IL-1β, IL-6, TNFα, and ANPEP), secreted by myeloid or lymphoid cells, was upregulated in the NO-NPs/fibrin hydrogels group (figure 9(b)). All of gene expression patterns shown in figure 9(d) indicate effects of NO treatment on mouse ovaries. Overall, NO/fibrin hydrogel treatment led to the preservation of ovarian follicles and tissue, which followed lymphangiogenesis in the transplanted ovaries to restore their function as reproductive organs.

4. Conclusion

Human ovarian tissue cryopreservation and transplantation is no longer an experimental method that is carried out in clinics to treat fertility preservation. However, ischemic injury due to lack of vessel anastomosis causes considerable ovarian follicle damage after transplantation. Therefore, we designed an NO-releasing nanoparticles/fibrin hydrogel complex with angiogenic potency to address ischemic injury and applied it for fertility preservation using a mouse model. The fibrin hydrogels act as support networks for transplanted mouse ovaries and nanoparticles, which have angiogenic potential. The NO/fibrin hydrogel improved the quality of tissue and mouse ovarian follicles; it also facilitated vasculature development. In addition, retrieved oocytes had the ability to become fertile by IVF with appropriate gene expression in transplanted ovaries. The technique proposed in this study can be applied to human OTT to reduce ischemic damage. However, further experiment with human ovarian tissue should be performed to confirm the beneficial effect before clinical application.

Data availability statement

The data that support the findings of this study are available upon reasonable request from the authors.

Acknowledgments

This research was supported by a grant of the Korea Health Technology R&D Project through the Korea Health Industry Development Institute (KHIDI), funded by the Ministry of Health & Welfare, Republic of Korea (Grant No. HI21C1353) and by a grant from the Bio & Medical Technology Development Program through the National Research Foundation of Korea (NRF) funded by the Ministry of Science and ICT (Grant Nos. NRF-2017M3A7B4049850, NRF-2016M3A9B4919711).

ORCID iDs

Kangwon Lee https://orcid.org/0000-0001-5745-313X
Jung Ryeol Lee https://orcid.org/0000-0003-3743-2934

References

[1] Resetkova N, Hayashi M, Kolp L A and Christianson M S 2013 Fertility preservation for prepubertal girls: update and current challenges *Curr. Obstet. Gynecol. Rep.* **2** 218–25
[2] Smith M A, Altekruse S F, Adamson P C, Reaman G H and Seibel N L 2014 Declining childhood and adolescent cancer mortality *Cancer* **120** 2497–506
[3] Spears N, Lopes F, Stefansdottir A, Rossi V, De Felici M, Anderson R A and Klinger F G 2019 Ovarian damage from chemotherapy and current approaches to its protection *Hum. Reprod. Update* **25** 673–93
[4] Oktay K and Karlikaya G 2000 Ovarian function after transplantation of frozen, banked autologous ovarian tissue *New Engl. J. Med.* **342** 1919
[5] Poirot C *et al* 2019 Impact of cancer chemotherapy before ovarian cortex cryopreservation on ovarian tissue transplantation *Hum. Reprod.* **34** 1083–94
[6] Kim S S, Battaglia D E and Soules M R 2001 The future of human ovarian cryopreservation and transplantation: fertility and beyond *Fertil. Steril.* **75** 1049–56
[7] Donnez J, Dolmans M M, Demylle D, Jadoul P, Pirard C, Squifflet J, Martinez-Madrid B and Van Langendonckt A 2004 Livebirth after orthotopic transplantation of cryopreserved ovarian tissue *Lancet* **364** 1405–10
[8] Revelli A, Marchino G, Dolfin E, Molinari E, Delle Piane L, Salvagno F and Benedetto C 2013 Live birth after orthotopic grafting of autologous cryopreserved ovarian tissue and spontaneous conception in Italy *Fertil. Steril.* **99** 227–30
[9] Demeestere I, Simon P, Dedeken L, Moffa F, Tsepelidis S, Brachet C, Delbaere A, Devreker F and Ferster A 2015 Live birth after autograft of ovarian tissue cryopreserved during childhood *Hum. Reprod.* **30** 2107–9
[10] Ernst E, Bergholdt S, Jorgensen J S and Andersen C Y 2010 The first woman to give birth to two children following transplantation of frozen/thawed ovarian tissue *Hum. Reprod.* **25** 1280–1
[11] Meirow D, Ra'anani H, Shapira M, Brenghausen M, Derech Chaim S, Aviel-Ronen S, Amariglio N, Schiff E, Orvieto R and Dor J 2016 Transplantations of frozen-thawed ovarian tissue demonstrate high reproductive performance and the need to revise restrictive criteria *Fertil. Steril.* **106** 467–74
[12] Silber S, Kagawa N, Kuwayama M and Gosden R 2010 Duration of fertility after fresh and frozen ovary transplantation *Fertil. Steril.* **94** 2191–6
[13] Abedi R, Eimani H, Pashaee Rad S, Eftekhari Yazdi P, Shahverdi A H and Mokhber Maleki E 2014 Evaluation effects of allopurinol and FSH on reduction of ischemia-reperfusion injury and on preservation of follicle after heterotopic auto-transplantation of ovarian tissue in mouse *Reprod. Med. Biol.* **13** 29–35
[14] Rafii S and Lyden D 2003 Therapeutic stem and progenitor cell transplantation for organ vascularization and regeneration *Nat. Med.* **9** 702–12
[15] Kong H S, Lee J, Youm H W, Kim S K, Lee J R, Suh C S and Kim S H 2017 Effect of treatment with angiopoietin-2 and vascular endothelial growth factor on the quality of xenografted bovine ovarian tissue in mice *PLoS One* **12** e0184546
[16] Youm H W, Lee J, Kim E J, Kong H S, Lee J R, Suh C S and Kim S H 2016 Effects of Angiopoietin-2 on transplanted mouse ovarian tissue *PLoS One* **11** e0166782
[17] Vong L B, Bui T Q, Tomita T, Sakamoto H, Hiramatsu Y and Nagasaki Y 2018 Novel angiogenesis therapeutics by redox injectable hydrogel—regulation of local nitric oxide generation for effective cardiovascular therapy *Biomaterials* **167** 143–52
[18] Yang C, Jeong S, Ku S, Lee K and Park M H 2018 Use of gasotransmitters for the controlled release of polymer-based nitric oxide carriers in medical applications *J. Control. Release* **279** 157–70
[19] Kargozar S, Baino F, Hamzehlou S, Hamblin M R and Mozafari M 2020 Nanotechnology for angiogenesis: opportunities and challenges *Chem. Soc. Rev.* **49** 5008–57
[20] Hu J, Fang Y, Huang X, Qiao R, Quinn J F and Davis T P 2021 Engineering macromolecular nanocarriers for local delivery of gaseous signaling molecules *Adv. Drug Deliv. Rev.* **179** 114005
[21] Lautner G, Meyerhoff M E and Schwendeman S P 2016 Biodegradable poly(lactic-co-glycolic acid) microspheres loaded with S-nitroso-N-acetyl-D-penicillamine for controlled nitric oxide delivery *J. Control. Release* **225** 133–9
[22] Blecher K *et al* 2012 Nitric oxide-releasing nanoparticles accelerate wound healing in NOD-SCID mice *Nanomedicine* **8** 1364–71
[23] Han G, Nguyen L N, Macherla C, Chi Y, Friedman J M, Nosanchuk J D and Martinez L R 2012 Nitric oxide-releasing nanoparticles accelerate wound healing by promoting fibroblast migration and collagen deposition *Am. J. Pathol.* **180** 1465–73
[24] Kang Y *et al* 2019 Tumor vasodilation by N-heterocyclic carbene-based nitric oxide delivery triggered by high-intensity focused ultrasound and enhanced drug homing to tumor sites for anti-cancer therapy *Biomaterials* **217** 119297
[25] Amirian J, Zeng Y, Shekh M I, Sharma G, Stadler F J, Song J, Du B and Zhu Y 2021 *In-situ* crosslinked hydrogel based on amidated pectin/oxidized chitosan as potential wound dressing for skin repairing *Carbohydr. Polym.* **251** 117005
[26] Amirian J, Linh N T, Min Y K and Lee B T 2015 Bone formation of a porous Gelatin-Pectin-biphasic calcium phosphate composite in presence of BMP-2 and VEGF *Int. J. Biol. Macromol.* **76** 10–24
[27] Amirian J, Sultana T, Joo G J, Park C and Lee B T 2020 *In vitro* endothelial differentiation evaluation on polycaprolactone-methoxy polyethylene glycol electrospun membrane and fabrication of multilayered small-diameter hybrid vascular graft *J. Biomater. Appl.* **34** 1395–408
[28] Kim J, Perez A S, Claflin J, David A, Zhou H and Shikanov A 2016 Synthetic hydrogel supports the function and regeneration of artificial ovarian tissue in mice *NPJ Regen. Med.* **1** 16010
[29] Day J R, David A, Cichon A L, Kulkarni T, Cascalho M and Shikanov A 2018 Immunoisolating poly(ethylene glycol)

based capsules support ovarian tissue survival to restore endocrine function *J. Biomed. Mater. Res.* A **106** 1381–9
[30] Basini G and Grasselli F 2015 Nitric oxide in follicle development and oocyte competence *Reproduction* **150** R1–9
[31] Laronda M M, Rutz A L, Xiao S, Whelan K A, Duncan F E, Roth E W, Woodruff T K and Shah R N 2017 A bioprosthetic ovary created using 3D printed microporous scaffolds restores ovarian function in sterilized mice *Nat. Commun.* **8** 15261
[32] Amorim C A and Shikanov A 2016 The artificial ovary: current status and future perspectives *Future Oncol.* **12** 2323–32
[33] Shikanov A, Zhang Z, Xu M, Smith R M, Rajan A, Woodruff T K and Shea L D 2011 Fibrin encapsulation and vascular endothelial growth factor delivery promotes ovarian graft survival in mice *Tissue Eng.* A **17** 3095–104
[34] Luyckx V, Dolmans -M-M, Vanacker J, Legat C, Fortuño Moya C, Donnez J and Amorim C A 2014 A new step toward the artificial ovary: survival and proliferation of isolated murine follicles after autologous transplantation in a fibrin scaffold *Fertil. Steril.* **101** 1149–56
[35] Chiti M C, Dolmans M M, Donnez J and Amorim C A 2017 Fibrin in reproductive tissue engineering: a review on its application as a biomaterial for fertility preservation *Ann. Biomed. Eng.* **45** 1650–63
[36] Yang C, Hwang H H, Jeong S, Seo D, Jeong Y, Lee D Y and Lee K 2018 Inducing angiogenesis with the controlled release of nitric oxide from biodegradable and biocompatible copolymeric nanoparticles *Int. J. Nanomed.* **13** 6517–30
[37] Lee J, Kong H S, Kim E J, Youm H W, Lee J R, Suh C S and Kim S H 2016 Ovarian injury during cryopreservation and transplantation in mice: a comparative study between cryoinjury and ischemic injury *Hum. Reprod.* **31** 1827–37
[38] Alibolandi M, Ramezani M, Sadeghi F, Abnous K and Hadizadeh F 2015 Epithelial cell adhesion molecule aptamer conjugated PEG-PLGA nanopolymersomes for targeted delivery of doxorubicin to human breast adenocarcinoma cell line *in vitro Int. J. Pharm.* **479** 241–51
[39] Alibolandi M, Sadeghi F, Abnous K, Atyabi F, Ramezani M and Hadizadeh F 2015 The chemotherapeutic potential of doxorubicin-loaded PEG-b-PLGA nanopolymersomes in mouse breast cancer model *Eur. J. Pharm. Biopharm.* **94** 521–31
[40] Liu J, Van der Elst J, Van Den Broecke R and Dhont M 2002 Early massive follicle loss and apoptosis in heterotopically grafted newborn mouse ovaries *Hum. Reprod.* **17** 605–11
[41] Smith R M, Shikanov A, Kniazeva E, Ramadurai D, Woodruff T K and Shea L D 2014 Fibrin-mediated delivery of an ovarian follicle pool in a mouse model of infertility *Tissue Eng.* A **20** 3021–30
[42] Cooke J P and Losordo D W 2002 Nitric oxide and angiogenesis *Circulation* **105** 2133–5
[43] Clapp C, Thebault S, Jeziorski M C and Martinez De La Escalera G 2009 Peptide hormone regulation of angiogenesis *Physiol. Rev.* **89** 1177–215
[44] Russell S J and Kahn C R 2007 Endocrine regulation of ageing *Nat. Rev. Mol. Cell Biol.* **8** 681–91
[45] Donnez J and Dolmans M M 2017 Fertility preservation in women *New Engl. J. Med.* **377** 1657–65
[46] Devesa J and Caicedo D 2019 The role of growth hormone on ovarian functioning and ovarian angiogenesis *Front. Endocrinol.* **10** 450
[47] Lee D M, Yeoman R R, Battaglia D E, Stouffer R L, Zelinski-Wooten M B, Fanton J W and Wolf D P 2004 Live birth after ovarian tissue transplant *Nature* **428** 137–8
[48] Demeestere I, Simon P, Emiliani S, Delbaere A and Englert Y 2007 Fertility preservation: successful transplantation of cryopreserved ovarian tissue in a young patient previously treated for Hodgkin's disease *Oncologist* **12** 1437–42
[49] Wu G and Scholer H R 2014 Role of Oct4 in the early embryo development *Cell Regen.* **3** 7
[50] Le Bin G C *et al* 2014 Oct4 is required for lineage priming in the developing inner cell mass of the mouse blastocyst *Development* **141** 1001–10
[51] Nath P and Maitra S 2019 Physiological relevance of nitric oxide in ovarian functions: an overview *Gen. Comp. Endocrinol.* **279** 35–44
[52] Dubey P K, Tripathi V, Singh R P and Sharma G T 2011 Influence of nitric oxide on *in vitro* growth, survival, steroidogenesis, and apoptosis of follicle stimulating hormone stimulated buffalo (Bubalus bubalis) preantral follicles *J. Vet. Sci.* **12** 257–65
[53] Yamamoto N, Oyaizu T, Enomoto M, Horie M, Yuasa M, Okawa A and Yagishita K 2020 VEGF and bFGF induction by nitric oxide is associated with hyperbaric oxygen-induced angiogenesis and muscle regeneration *Sci. Rep.* **10** 2744
[54] Brown H M and Russell D L 2014 Blood and lymphatic vasculature in the ovary: development, function and disease *Hum. Reprod. Update* **20** 29–39
[55] Van Eyck A-S, Bouzin C, Feron O, Romeu L, Van Langendonckt A, Donnez J and Dolmans M-M 2010 Both host and graft vessels contribute to revascularization of xenografted human ovarian tissue in a murine model *Fertil. Steril.* **93** 1676–85
[56] Gaharwar A K, Singh I and Khademhosseini A 2020 Engineered biomaterials for *in situ* tissue regeneration *Nat. Rev. Mater.* **5** 686–705